

RESEARCH

Open Access



# Tritium labeling of antisense oligonucleotides via different conjugation agents

Martin R. Edelmann<sup>1,2\*</sup> , Christophe Husser<sup>3</sup>, Martina B. Duschmalé<sup>3</sup>, Guy Fischer<sup>3</sup>, Claudia Senn<sup>3</sup>, Erich Koller<sup>3</sup> and Andreas Brink<sup>3</sup>

## Abstract

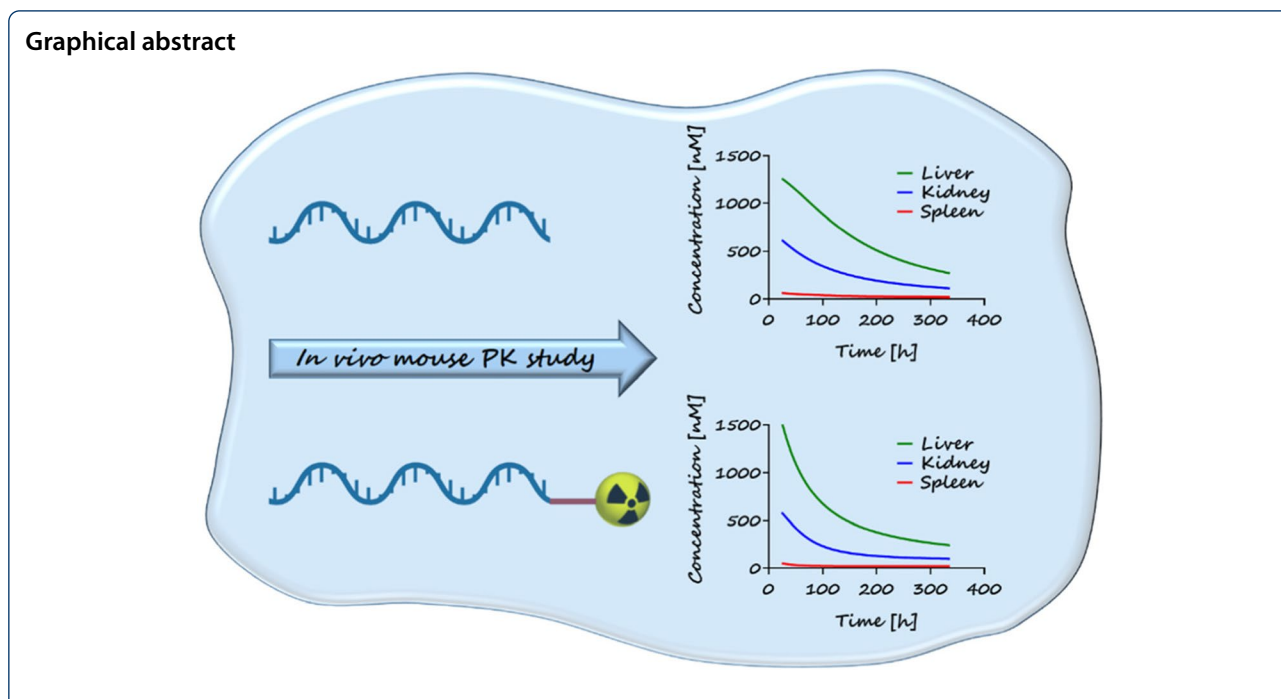
A novel approach to tritium-labeled antisense oligonucleotides (ASO) was established by conjugating *N*-succinimidyl propionate, as well as maleimide-derivatives, to the 3'-end of ASOs targeting metastasis-associated lung adenocarcinoma transcript 1 (Malat1) containing amino- or sulfhydryl-linkers. In vitro stability and Malat1 RNA reduction studies demonstrated that *N*-ethylmaleimide (NEM) could be used as a stable tag while maintaining the desired target interaction. The corresponding radioactive label conjugation using [<sup>3</sup>H]-NEM resulted in tritium-labeled ASOs with a high molar specific activity of up to 17 Ci/mmol. Single-dose in vivo studies in mice were carried out to compare [<sup>3</sup>H]-ASOs with their unlabeled counterpart ASOs, with and without conjugation to *N*-acetylgalactosamine (GalNAc), for tissue and plasma concentrations time profiles. Despite the structural modification of the labeled ASOs, in vitro target interaction and in vivo pharmacokinetic behaviors were similar to that of the unlabeled ASOs. In conclusion, this new method provides a powerful technique for fast and safe access to tritium-labeled oligonucleotides, e.g., for pharmacokinetic, mass balance, or autoradiography studies.

**Keywords:** Antisense oligonucleotide, Radiolabeling, Malat1, Pharmacokinetics, Tritium

\*Correspondence: martin.edelmann@roche.com

<sup>2</sup> Roche Pharma Research and Early Development, Therapeutic Modalities, Roche Innovation Center Basel, F. Hoffmann-La Roche Ltd, Grenzacherstr. 124, CH-4070 Basel, Switzerland

Full list of author information is available at the end of the article



## Introduction

The transcription of DNA to RNA and subsequent translation to functional proteins is a central element in living cells. Using viral RNA, Stephenson and Zamecnik (1978) demonstrated in 1978 that translation of proteins could be efficiently inhibited *in vitro* by competitive hybridization with antisense oligonucleotides (ASO). Today, there are several approved ASO-based therapies, such as Spinraza (Ionis/Biogen), Waylivra (Ionis/Akcea/PTC), and Exondys (Sarepta Therapeutics), available on the market (Wang et al. 2020). There is growing interest across the pharmaceutical industry to discover and develop new ASO-based therapies, employing various mechanisms to inhibit mRNA translation, e.g., formation of ASO/RNA complexes that activate RNase H, which degrades the mRNA or prevents ribosome recruitment (Muntoni and Wood 2011). ASOs are also used to modify splicing or to increase protein expression by targeting upstream open reading frames (Havens and Hastings 2016; Sasaki et al. 2019). As with small molecule drugs throughout the drug development process from preclinical to clinical studies, regulatory data packages for ASOs are required to demonstrate safety, efficacy, and tolerability of the new drug as well. The use of radiolabeled compounds allows a mechanistic and quantitative understanding of the fate of ASO in the body with the aim to characterize them and further optimize their absorption, distribution, metabolism, and excretion (ADME) properties. Often, carbon-14 is used to label small molecule drug candidates, since it

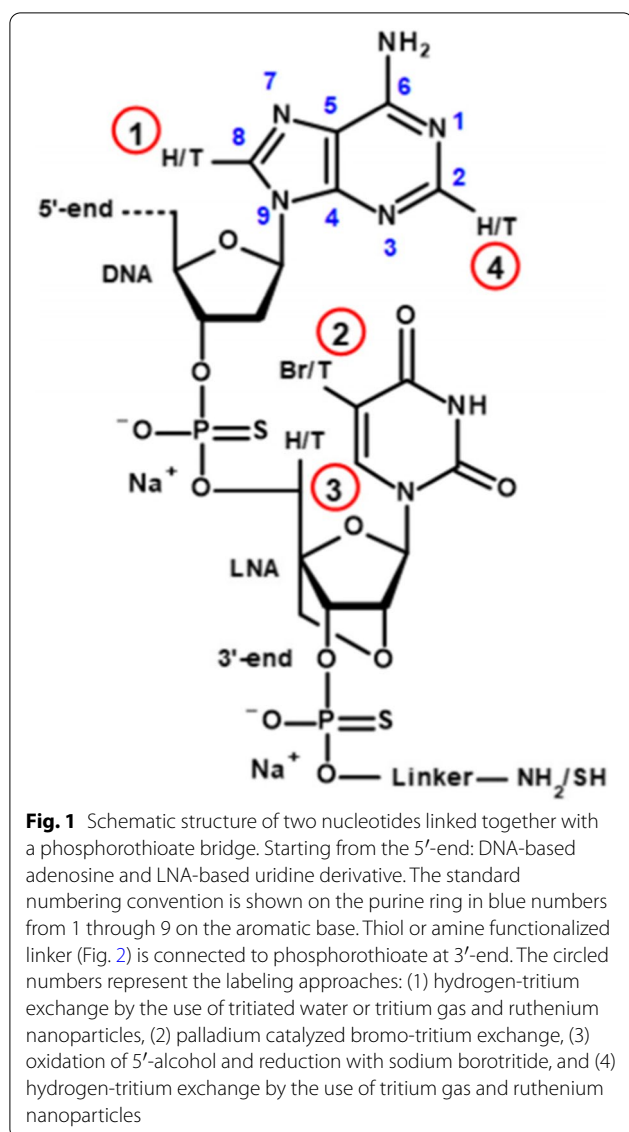
can be introduced in a metabolically stable position. For larger molecules such as oligonucleotides, however, the resulting molar specific activity after carbon-14 (62.4 mCi/mmol) labeling might be insufficient for a quantitative determination by liquid scintillation counting (LSC). Tracing of carbon-14 is possible by accelerated mass spectrometry (AMS), but this technology requires special equipment.

Therefore, tritium (molar specific activity: 26.6 Ci/mmol;  $t_{1/2}$ : 12.3 y) was preferred over carbon-14 as a radioisotope for the ASO study, as the molar specific activity of tritium is about 430 times higher than that of carbon-14.

Various approaches have already been published to incorporate tritium into an oligonucleotide. In a bio-transformation study described by Shemesh and colleagues (Shemesh et al. 2016), tritium was introduced into a linker that connects an ASO and a targeting moiety (GalNAc). These radiolabeled ASO constructs were compared to the corresponding cold (non-radioactive) ASOs and showed similar *in vivo* behavior.

Lesnik and co-workers (Graham et al. 1993) described a hydrogen-tritium exchange in tritiated water at the C8 position in purines (Fig. 1 (1)). The rapid tritium exchange at the C8 position back to hydrogen does not allow for longer-term *in vivo* studies.

Another procedure for small interfering RNAs (siRNA) was based on inserting 5-bromouridine derivatives (Fig. 1 (2)) into the sequences followed by



a halogen-tritium exchange by palladium-catalyzed hydrogenation with tritium gas (Christensen et al. 2012). The transfer of this approach to oligonucleotides containing phosphorothioate backbones was not successful, even with a high number of equivalents (> 100) of “catalyst”.

A different reported approach requires the oxidation of the 5'-terminal primary alcohol of nucleotide monomers, and, in a second step, reduction of the aldehydes with a tritium-labeled reducing agent such as NaBT<sub>4</sub> (Tan et al. 1997). After multiple steps, involving 3'-phosphoramidite activation of the nucleotide, the tritium-labeled monomers can then be used for building up the desired oligonucleotide (Fig. 1 (3)). The key issue of this approach is the instability of the

tritium-labeled nucleotide-phosphoramidite, which leads to low yields, high radioactive waste, and low specific activity of the final product.

Palazzolo et al. (2019) demonstrated a random hydrogen/tritium exchange on a 6-mer or 12-mer DNA-based oligonucleotide containing phosphate backbones under tritium gas and catalyzed with ruthenium nanoparticles. The reported exchange took place exclusively in purine rings at the C2 and C8 positions (Fig. 1 (1, 4)). As already mentioned, the risk of a re-exchange at C8 position to hydrogen is possible. To the best of our knowledge, a feasibility with a phosphorothioate-based oligonucleotide has not yet been reported. A general disadvantage of a random labeling technique is that the quantification of radioactively labeled oligonucleotides in metabolism studies is very difficult or even impossible, as the label is distributed evenly over the entire molecule.

Generally, radiolabeling of ASO molecules is not straightforward. Robust tritium-labeling techniques are not readily available and thus often represent a bottleneck in pre-clinical ASO research. There is an urgent need for efficient approaches to increase the availability of radiolabeled ASOs for pre-clinical and clinical research.

To find new efficient ways to increase availability of tritium-labeled ASOs, a novel strategy was studied to conjugate pre-labeled tags via different linkers to the 3'-end using experimental oligonucleotides containing locked nucleic acids (LNAs) (Hagedorn et al. 2018).

First, we evaluated the feasibility of labeling concepts by conjugating different tags to functionalized linkers of oligonucleotides. Second, we investigated the metabolic stability and in vitro potency by target reduction of tagged tool-ASOs in human and mouse hepatocytes in comparison to their untagged analogs. Finally, to verify the in vivo applicability of our approach, we conducted a PK study in mice using two tritium-labeled oligonucleotides to study ASO distribution into different tissues following subcutaneous administration.

The key questions that we addressed in this study were whether tritium bioconjugation on functionalized ASOs is feasible and whether this modification has an influence on the stability, RNA reduction, or biodistribution compared to their congeners.

## Materials and methods

### Chemicals and equipment

All oligonucleotides, which were used as starting materials, were synthesized by Roche Pharma Research and Early Development using standard phosphoramidite chemistry. Modifiers were incorporated at the start of the synthesis by placing the amino or thiol-group at the 3'-end using 3'-Amino-Modifier TFA Amino C-6 Ica CPG (Hauppauge, NY, USA) and 3'-Thiol-Modifier C<sub>6</sub>

S-S (GLEN Research, Sterling, VA, USA). *N*-Succinimidyl propionate (NSP) (Wako), *N*-methylmaleimide (NMM) (Fluka), and *N*-ethylmaleimide (NEM) (Fluka) are commercially available and have been used without further purification. Phosphate-buffered saline (PBS) was purchased from Thermo Fisher Scientific (Paisley, UK). PBS contained 1.54 mM potassium phosphate monobasic, 2.71 mM potassium phosphate dibasic, and 155.17 mM sodium chloride. Tritium-labeled *N*-[<sup>3</sup>H]ethylmaleimide (molar activity: 2 TBq/mmol = 55 Ci/mmol) was obtained from Pharmaron (Cardiff, Wales, UK) as a solution in pentane. Liquid scintillation counting (LSC) for tritium compounds was accomplished using a HIDEX 300 SL and ULTIMATE GOLD cocktail (PerkinElmer Inc., Waltham, MA, USA). Reaction monitoring and purity for NSP conjugations on amine-linkers were determined by HPLC Agilent 1210 at 260 nm wavelength, Waters XBridge RP18, 4.6 × 150 mm, 3.5 μm column at 60 °C ([A] = water/methanol/hexafluoro *i*-propanol/TEA : 950/25/21/2.3 mL; [B] = water/methanol/hexafluoro *i*-propanol/TEA: 175/800/21/2.3 mL, at a flow rate of 1.0 mL/min with the following gradient: 10% [B] to 60% [B] in 12 min). Conjugations with maleimide derivatives were determined by UPLC Agilent 1290 at 260 nm wavelength, ACQUITY UPLC Oligonucleotide BEH C18, 2.1 × 50 mm, 1.7 μm column at 80 °C with the same eluents and the following gradient: 10% [B] to 40% [B] in 6 min. Radiochemical purity was measured using the β-radioactivity HPLC detector RAMONA Quattro with an internal solid scintillator (Raytest, Straubenhardt, Germany). Mass spectrometry analysis was performed using a Thermo Fisher Scientific (Waltham, MA, USA) Vanquish UHPLC System, Orbitrap Fusion Lumos Tribrid, and a Waters ACQUITY Oligonucleotide BEH C18 (2.1 × 50 mm, 1.7 μm) column in negative-ion mode. MS (m/z) was calculated from the multiply charged peak pattern. Preparative HPLC for NSP conjugation was performed using a Gilson PLC 2050 (Mettmenstetten, CH) with an XBridge C18 column, 5 μm, 10 × 250 mm and using water (950 mL)/methanol (25 mL)/TEA (2.3 mL)/hexafluoro *i*-propanol (21 mL) as mobile phase [A] and water (175 mL)/methanol (800 mL)/TEA (2.3 mL)/hexafluoro *i*-propanol (21 mL) as mobile phase [B] in gradient elution with 10% [B] to 60% [B] in 15 min. Concentration was determined using a Eppendorf Bio-Spectrometer® basic (Hamburg, Germany) at 260 nm wavelength and the corresponding calculated molar extinction coefficient. In order to determine the specific activity of tagged ASOs, the activity concentration [mCi/mL] of oligonucleotide solution was determined by LSC and divided by the content concentration [mg/mL] to give the specific activity in mCi/mg. Based on

the molecular weight, the molar specific activity in Ci/mmol could be calculated for each tagged ASO.

#### Labeling procedures

##### Labeling procedure I: NSP conjugation on amino-linker

Four milligrams (0.73 μmol) of ASO 2-precursor, containing 3'-end amino-linker, was dissolved in 0.5 mL *N,N*-dimethylformamide 5 μL (29.06 μmol) Hünig's base and 150 μg (0.87 μmol) *N*-succinimidyl propionate, dissolved in 60 μL *N,N*-dimethylformamide, were added to give a colorless suspension. The mixture was stirred for 16 h at 22 °C to become a clear solution. The solvent was removed under high vacuum and the residue dissolved in PBS. Crude mixture was purified by preparative HPLC. The desired fractions were transferred into an Amicon® Pro purification system (MWCO: 3,000 Da) and centrifuged at 4,000 rpm. Deionized water was added, and the process was repeated 4 more times to complete the exchange from HPLC eluent to water. The resulting aqueous solution lyophilized to isolate 3.0 mg (74%) of ASO 2 as a colorless powder with a purity of 95%. MS (m/z): 5,561.6 [M-(H)]<sup>-</sup>.

##### Labeling procedure II: maleimide derivatives conjugation on sulfhydryl-linker

Four milligrams (0.73 μmol) of ASO 3-precursor, containing 3'-end sulfhydryl linker, was dissolved in 1 mL PBS. (127 μg, 1.14 μmol) *N*-methyl maleimide, dissolved in 61 μL dimethyl sulfoxide, was added to the aqueous solution and stirred at 22 °C for 16 h. UPLC analysis showed a complete addition of maleimide to the oligonucleotide. To exchange the buffer to water, the reaction mixture was transferred into an Amicon® Pro purification system (MWCO: 3,000 Da) and centrifuged at 4000 rpm. Deionized water was added, and the process was repeated 4 more times to complete the exchange. The resulting aqueous solution was lyophilized to isolate 2.8 mg (69%) of the desired oligonucleotide as a colorless powder with purity of 97%. MS (m/z): 5602.2 [M-(H)]<sup>-</sup>.

ASOs 4 and 6 were prepared in a similar manner according to the "Labeling procedure II: maleimide derivatives conjugation on sulfhydryl-linker" section:

ASO 4: Yield: 73%, purity: 96%, MS (m/z): 5616.2 [M-(H)]<sup>-</sup>

ASO 6: Yield: 73%, purity: 99%, MS (m/z): 7833.4 [M-(H)]<sup>-</sup>

##### Labeling procedure III: [<sup>3</sup>H]-*N*-ethylmaleimide ([<sup>3</sup>H]-3) conjugation on sulfhydryl-linker

30 mCi (1.1 GBq) of *N*-[<sup>3</sup>H]ethyl maleimide ([<sup>3</sup>H]-3, 61.5 μg, 0.477 μmol) in 12 mL pentane was concentrated on a silica gel pre-packed column and eluted with 2 × 0.5 mL

DMSO. A solution of 2.20 mg (0.401  $\mu\text{mol}$ ) ASO 7-precursor in 1 mL PBS was added and stirred for 1 h at 22 °C. UPLC analysis showed 40% of the desired product and 60% of unreacted starting material. Non-radioactive NEM (502  $\mu\text{g}$ , 4.01  $\mu\text{mol}$ ) was added and stirred for 1 h at 22 °C. UPLC showed a complete addition to the desired product. The reaction solution was transferred into a 5 mL Float-A-Lyzer<sup>®</sup> tube (MWCO: 500–1000 Da) and dialyzed against PBS pH 7.1 at 22 °C. The buffer was changed 4 times after 45 min and stored 16 h in the fridge. UPLC analysis showed a high polar radio impurity. The solution was filled into an Amicon<sup>®</sup> Pro purification system (MWCO: 3000 Da) and centrifuged at 4000 rpm. PBS was added and the process was repeated 4 more times to achieve a radiochemical purity of 99%. Isolated amount: 1.58 mg (yield: 70%), isolated radioactivity: 4.4 mCi (163 MBq), radiochemical yield: 15%, specific activity: 2.8 mCi/mg (104 MBq/mg) which is equal to 16.6 Ci/mmol (614 MBq/mmol).

ASO 8 was prepared in a similar manner according to the “Labeling procedure III: [<sup>3</sup>H]-*N*-ethylmaleimide ([<sup>3</sup>H]-3) conjugation on sulfhydryl-linker” section:

ASO 8: Yield: 92%, isolated radioactivity: 0.9 mCi, radiochemical yield: 9%, radiochemical purity: 93%, specific activity: 1.8 mCi/mg (67 MBq/mg), molar specific activity: 13.0 Ci/mmol (481 GBq/mmol).

#### Cell culture, oligonucleotide treatment, mRNA isolation, and qPCR

Mouse hepatocytes were isolated from C57BL/6 mice by a two-step collagenase liver perfusion method as previously described (Sewing et al. 2016). Freshly isolated primary mouse hepatocytes were plated in collagen-I-coated 96-well plates and treated in Williams Medium E containing 10% fetal bovine serum without antibiotics. Cells were treated with LNA solutions in the indicated concentrations in full cell culture medium about 1 h after plating for an incubation time of 3 h. Then the cells were washed 3 times with PBS containing  $\text{Ca}^{2+}$  and  $\text{Mg}^{2+}$  and incubated in fresh cell culture medium without the oligonucleotide compound. After 21 or 69 h, hepatocytes were washed 3 times with PBS containing  $\text{Ca}^{2+}$  and  $\text{Mg}^{2+}$  and lysed with 135  $\mu\text{L}$  PureLink Pro lysis buffer. Five, 10, and 20  $\mu\text{L}$  were sampled for hybridization based ELISA assay as described earlier (Straarup et al. 2010) and 100  $\mu\text{L}$  was used for mRNA purification using the PureLink Pro 96 RNA Kit from Thermo Fisher Scientific. One Step RT-qPCR for Malat1 mRNA levels was performed, respectively. mRNA levels were normalized to the total RNA amount quantified with Ribogreen QuantIT (Thermo Fisher Scientific). Total RNA was isolated using the PureLink Pro 96 RNA Kit from Thermo

Fisher Scientific according to the manufacturer’s instructions and RT-qPCR was performed using the LightCycler Multiplex RNA Virus Master (Roche) with primer probe sets (all from Thermo Fisher Scientific) human Malat1 (Hs00273907\_s1), mouse Malat1 (Mm01227912\_s1). The obtained data was normalized to total RNA amounts determined via Ribogreen quantification. All data points were performed in triplicate, and data are given as the average.  $\text{IC}_{50}$  values were fitted with GraphPad Prism with a constrained HillSlope set to 1. Results are reported as  $\text{IC}_{50}$  value  $\pm$  standard deviation.

#### In vivo mouse study

The study was conducted with the approval of the local veterinary authority with strict adherence to the Swiss federal regulations on animal protection and to the rules of the Association for Assessment and Accreditation of Laboratory Animal Care International (AAALAC).

#### Animals and housing conditions

Male C57BL/6 J mice ( $n = 24$ , 8 to 12 weeks old) were purchased from Charles River Laboratories, France. The mice were group housed in open cages and maintained on a 12:12-h light:dark cycle, with constant temperature (21–24 °C) and humidity (40–80%). Each cage was provided with unrestricted access to municipal water and sterilized food (Provimi Kliba 3436). All cages (except metabolism cages) were supplied with autoclaved sawdust bedding and environmental enrichments, which were applied to best practice animals’ welfare standards and rotated weekly. The mice were acclimated for at least 1 week before the start of the study.

#### Study design

The mice were randomly allocated into 4 groups ( $n = 6$  per group) according to the 4 different compounds. The compounds were formulated as a solution in Dulbecco’s PBS (pH 7) and administered subcutaneously as a single dose of 1 mg/kg of body weight (dosing volume of 4 mL/kg). In a composite sampling design, blood (100  $\mu\text{L}$ /time point/mouse) was collected sublingually from mice under deep anesthesia with 5% isoflurane in pure oxygen. Blood was collected at 15 min, 1 h, 4 h, 24 h, 48 h, and 72 h post dose into EDTA-coated polypropylene tubes followed by plasma separation by centrifugation at 15,000 rpm for 5 min at 4 °C. Urine samples were collected post injection by thoroughly rinsing the collection surface with 3 mL distilled water. For excretion collections, mice were housed in pairs in metabolic cages during 0–24 h, 24–48 h, and 48–72 h intervals post administration. Organs and plasma were collected at terminal time points of 1 day, 3 days, and 14 days after pentobarbital-induced anesthesia (40 mg/kg, i.p.). Plasma samples were stored at  $-20$

°C for further processing and analysis. Samples of liver, kidney, and spleen were collected into homogenization tubes (Precellys® CK28, Bertin Instruments, France).

### Bioanalytics

#### **Quantitative exposure assessment of full-length compounds**

Tissue samples were collected and weighed during necropsy and stored at  $-80^{\circ}\text{C}$  in homogenization tubes CK28 (Precellys®) for subsequent bioanalytical examination by LC coupled to tandem mass spectrometry (LC-MS/MS). Prior to extraction tissue homogenates were diluted 5-fold in mouse blank plasma. The quantification was performed against a mouse plasma calibration curve. Calibration ranges were 0.267–666 nM for ASO 1 and 0.380–950 nM for ASO 5, respectively.

Fifty microliters of calibration standards, quality control samples (freshly prepared in mouse plasma), and tissue homogenate samples diluted in mouse blank plasma were treated for protein denaturation with 150  $\mu\text{L}$  of 4 M guanidine thiocyanate after addition of the internal standard (2000 ng/mL). A characterized 16-mer oligonucleotide (MW: 5460 Da), consisting of DNA nucleotides, LNA nucleotides, and a complete phosphorothioate backbone, was used as an internal standard in order to exclude possible variations during pipetting, solid-phase work-up, or LC-MS/MS sample injections. After vigorously mixing (20 min at 1,600 rpm), 200  $\mu\text{L}$  of a  $\text{H}_2\text{O}$ /HFIP/DIPEA solution (100:4:0.2, v/v/v) were added, followed by mixing (15 min at 1500 rpm). Then, a clean-up step was performed using solid-phase-extraction cartridges (Waters, OASIS HLB, 30  $\mu\text{m}$ ) after elution and evaporation to dryness (30–45 min at  $40^{\circ}\text{C}$ ) the samples were reconstituted in 200  $\mu\text{L}$  of mobile phase ( $\text{H}_2\text{O}$ /MeOH/HFIP/DIPEA [95/5/1/0.2, v/v/v/v]). After vortex mixing (10 min at 1500 rpm), an aliquot (20  $\mu\text{L}$ ) was injected into the analytical column (Waters, Acquity BEH C18, 1.7  $\mu\text{m}$ ,  $50 \times 2.1$  mm kept at  $60^{\circ}\text{C}$ ). The analyte and internal standard were separated from matrix interferences using gradient elution from  $\text{H}_2\text{O}$ /MeOH/HFIP/DIPEA (95/5/1/0.2, v/v/v/v) to  $\text{H}_2\text{O}$ /MeOH/HFIP/DIPEA (10/90/1/0.2, v/v/v/v) within 4 min at a flow rate of 0.4 mL/min. Mass spectrometric detection was carried out on an AB-Sciex 6500+ mass spectrometer using selected reaction monitoring (SRM) in the negative-ion mode. The selected ion reactions (m/z) were 680.6/94.8 and 658.9/94.8 for ASO 1 and ASO 5 respectively and 596.1/94.8 for Internal Standard. Detection was accomplished utilizing ion spray MS/MS in negative ion SRM mode.

In the case of animals dosed with GalNAc-conjugated compounds (ASO 5 and ASO 8), total or partial cleavage of the GalNAc moiety was expected; therefore, we measured both the intact compound (with GalNAc) and also

the naked moiety (corresponding to ASO 1 and ASO 7, respectively), in order to quantify the amount of GalNAc-cleavage compounds.

#### **Determination of total radioactivity by liquid scintillation counting**

Plasma, urine, and fecal extract were analyzed using liquid scintillation analysis. To enable scintillation analysis, aliquots of each sample (typically 20–200  $\mu\text{L}$ ) were mixed with Ultima Gold liquid scintillation cocktail (5 mL; PerkinElmer) in plastic scintillation vials (7 mL; PerkinElmer) and analyzed using a Radiomatic 150TR flow or Tri-Carb 3100 TR scintillation analyzer with automatic quench correction against an external standard (PerkinElmer, Waltham, MA, USA). Further manipulation of the raw data and conversion to concentrations were performed on spreadsheets running on Microsoft Excel 2010.

#### **Metabolite identification in vitro and in vivo**

For in vitro studies of metabolism, hepatocyte cell pellets were collected from the hepatocytes incubations described above. For in vivo metabolism studies, liver, kidney, and spleen tissue samples were collected after necropsy in the described in vivo study and were stored at  $-80^{\circ}\text{C}$  in homogenisation tubes CK28 (Precellys®). Tissue homogenates and hepatocyte lysates were prepared by adding 300  $\mu\text{L}$  of  $\text{H}_2\text{O}$  to 100 mg of tissue or to hepatocyte samples, respectively, followed by mixing the CK28 tubes in the Precellys homogenizer. The analysis of biotransformation of the oligonucleotide compounds in the resulting tissue homogenates and cell lysates was performed as described previously (Husser et al. 2017; Husser et al. 2019). In brief, 50  $\mu\text{L}$  of homogenate or cell lysate were mixed with 250  $\mu\text{L}$  of guanidine thiocyanate 4 M in 0.1 M Tris buffer pH 7.5 for 15 min at  $25^{\circ}\text{C}$  in a Thermo mixer. Then, 700  $\mu\text{L}$   $\text{H}_2\text{O}$ /HFIP/DIPEA 100/2/0.2 v/v/v were added and mixed for 1 h at  $25^{\circ}\text{C}$ . Four to 8  $\mu\text{L}$  of internal standard (ISTD) 20–1000  $\mu\text{M}$  in  $\text{H}_2\text{O}$ /MeOH/HFIP/DIPEA 100/10/1/0.1 v/v/v/v were added, and the sample centrifuged for 5 min at 14,000 rpm. Subsequently, the supernatant was subjected to a solid phase extraction (SPE) OASIS HLB 1 cc 30 mg cartridge (Waters, Wexford, Ireland) followed by analysis with LC-HRMS. A Thermo Scientific Dionex UltiMate NCP-3200RS Binary Rapid Separation HPLC system was used in combination with a Pal autosampler (CTC Analytics AG, Zwingen, Switzerland), and a Thermo Scientific Orbitrap Fusion Tribrid Mass Spectrometer (Thermo Scientific, Bremen, Germany) equipped with an electrospray ionization (ESI) source. The oligonucleotide metabolites were analyzed in negative-ionization mode using a full scan MS experiment combined with two parallel MS<sup>2</sup>

experiments, one data-dependent scan and an untargeted all-ion fragmentation (AIF) experiment applying high collision energy. In the AIF scan, a diagnostic fragment originating from the phosphorothioate backbone ( $\text{O}_2\text{PS}^-$ :  $m/z$  94.936) was formed efficiently upon collisional activation. Based on this fragment an accurate determination of metabolites of oligonucleotides was achieved, independent of their sequence in an untargeted but highly selective manner. MS data were analyzed using XCalibur software (Thermo Scientific, Bremen Germany). MS intensities were recorded as the sum of the most intense charge states of the most intense isotopes of the respective analyte applying an  $m/z$  window of 5 ppm.

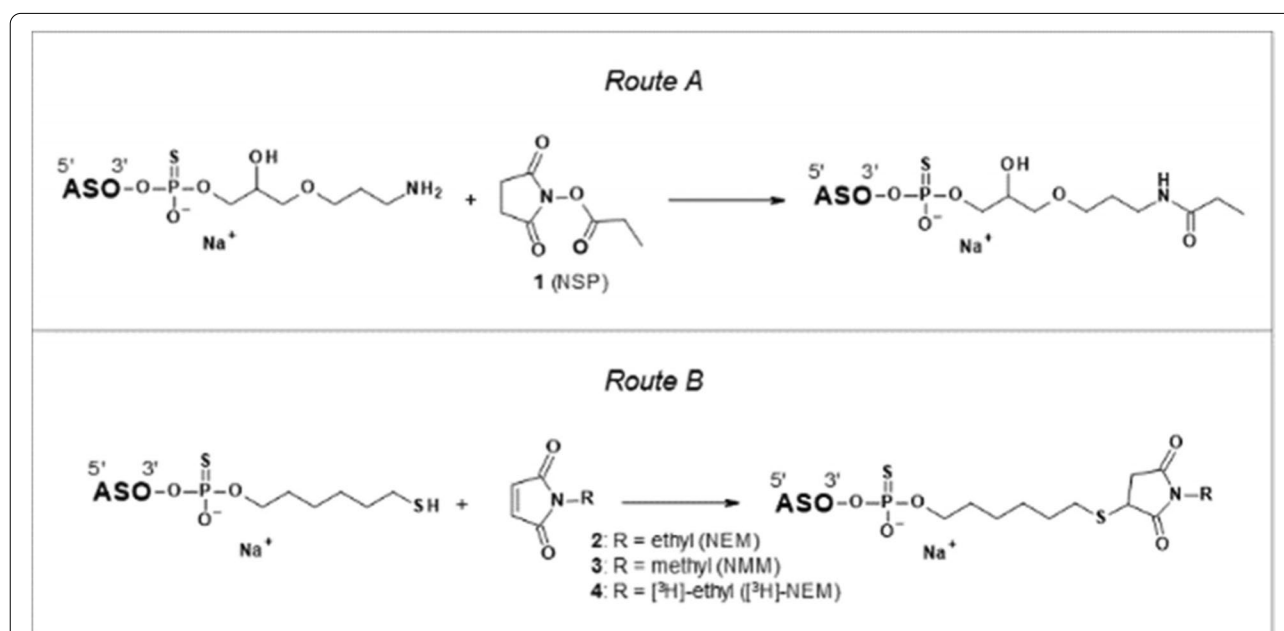
## Results

### Conjugation methods

To develop radiolabeling strategies for ASOs, the feasibility of labeling on functionalized linkers that are attached to ASOs was investigated. In the study, we selected experimental-ASOs that contain LNA, DNA monomers, and phosphorothioate backbones. Standard LNA-incorporating ASOs are usually based on single-stranded 14–20-mers and contain three structural units: LNA nucleotides, DNA nucleotides, and a phosphorothioate backbone. A comparative study has shown that LNA-modified ASOs display a 10-fold higher human serum stability compared to unmodified DNA counterparts. Furthermore, LNAs manifested an

improved nuclease resistance, which results in a higher metabolic stability in vivo (Grünweiler and Hartmann 2007).

Two labeling routes (*Route A*, *Route B*), which highlight the two types of linkers for subsequent labeling conjugations are shown in Fig. 2. The introduction of a propionyl residue using *N*-succinimidyl propionate (NSP) is described in the section “Labeling procedure I: NSP conjugation on amino-linker” (*Route A*). In brief, NSP was introduced at the 3'-end of the ASO via an aminopropyl glycerol-based linker in *N,N*-dimethylformamide and Hünig's base. The crude conjugate was purified by preparative HPLC in a yield of 74 % and purity of 95%. The section “Labeling procedure II: maleimide derivatives conjugation on sulfhydryl-linker” (*Route B*) describes the maleimide-based conjugation to the thiol-linker at the 3'-end. Conjugations with both, *N*-methylmaleimide (NMM) or alternatively *N*-ethylmaleimide (NEM) were achieved. Actual tritiated oligonucleotides used for this study were only prepared with [ $^3\text{H}$ ]-NEM as described in the section “Labeling procedure III: [ $^3\text{H}$ ]-*N*-ethylmaleimide ([ $^3\text{H}$ ]-3) conjugation on sulfhydryl-linker” (*Route B*). Each maleimide-based conjugation was carried out in an aqueous phosphate buffer and worked-up using ultra-centrifugal filtration. Recovery yields up to 92% and purities of > 93% could be achieved with molar specific activities in the range of 13 to 17 Ci/mmol.



**Fig. 2** Overview of different approaches applied in this study to introduce tritium labels to oligonucleotides by conjugation. Introducing propionyl using (1) *N*-succinimidyl propionate (NSP) to the 3'-end via an aminopropyl glycerol-based linker (*Route A*), and via Michael addition of (2) *N*-ethylmaleimide (NEM), (3) *N*-methylmaleimide (NMM), or (4) *N*-[ $^3\text{H}$ ]ethylmaleimide ([ $^3\text{H}$ ]-NEM) to a  $\text{C}_6$ -thiol-linker at the 3'-end (*Route B*)

The labeling with [<sup>3</sup>H]-NEM was a challenge when preparing for conjugations, as the radioactive tracer was supplied in a pentane solution. Evaporation of the solvent was not possible because NEM easily sublimates, and this led to a simultaneous loss of the radioactive maleimide derivative. This could be addressed by a solvent exchange to a water-soluble solvent. The pentane solution was applied to a short silica-based column, the solvent was removed from the column using a stream of argon, and the remaining [<sup>3</sup>H]-NEM was eluted with DMSO.

We hypothesize that the use of DMSO during the synthesis led to a partial sulfur/oxygen exchange in the phosphorothioate-backbone of the oligonucleotide. We observed side products in the synthesis product with mass shifts (−16 Da) that were consistent with the exchange of sulfur to oxygen. Based on MS signal intensity and semi-quantification by MS peak areas, a ratio of no exchange (38%) to 1x S/O exchange (−16 Da; 41%) to 2x S/O exchange (−32 Da; 21%) was observed for ASO 7. For ASO 8, the exchange was less pronounced: no exchange (62%), 1x S/O exchange (30%), and 2x S/O exchange (8%). A similar exchange was not observed in the non-radioactive conjugations, possibly because significantly less DMSO was used in the “Labeling procedure II: maleimide derivatives conjugation on sulfhydryl-linker” section. The conjugation to ASO 6 was therefore carried out under the same conditions as described in the “Labeling procedure III: [<sup>3</sup>H]-*N*-ethylmaleimide ([<sup>3</sup>H]-3) conjugation on sulfhydryl-linker” section. In this case, a mass spectrometric analysis showed an S/O exchange in the ratio of no exchange (78%) to 1x S/O exchange (−16 Da, 19%) to 2x S/O exchange (−32 Da, 3%) which is similar to the mass pattern of the corresponding radiolabeled ASO 8. These findings support the hypothesis that there is a correlation between the use of DMSO and an S/O exchange. As a result of the S/O exchange that occurred, the molecular weight changed, and tissue concentrations of tritium-labeled oligonucleotides could not be determined by LC-MS/MS using the reference compounds. Radioactivity measurements, however, were feasible so that ASO concentrations in tissues could be compared with untagged counterparts.

Table 1 provides an overview of synthesized oligonucleotide constructs used for in vitro and in vivo studies. Single-stranded ASO sequences of metastasis-associated lung adenocarcinoma transcript 1 (Malat1; 16-mer) were conjugated with non-radioactive tags for assessing stability and target reduction in vitro. In addition, the Malat1 oligonucleotide was also tested as its *N*-acetylgalactosamine (GalNAc) conjugate. Conjugations of ASOs to GalNAc have been shown to shift their biodistribution from Kupffer cells towards hepatocytes in liver tissue via high-affinity binding to the asialoglycoprotein receptor

**Table 1** Overview of oligonucleotides used in different proof-of-concept studies. Capital letters in sequence describe LNA-modified nucleosides, small letters describe DNA nucleosides. *GN*: GalNAc, *AmC<sub>6</sub>*: amino hexylene, *GBB-Am*: aminopropyl glycerol based bridge, *C<sub>6</sub>SH*: hexylene sulfhydryl, *NSP*: *N*-succinimidyl propionate, *NMM*: *N*-methylmaleimide, *NEM*: *N*-ethylmaleimide, *i*: in vitro target reduction and MetID, *ii*: in vivo mouse PK study. Column “Study” describes the use of oligonucleotides in different studies

ASO	Oligonucleotide sequence 5' → 3'	Linker	Adduct	Study
1	5'-GAGTtacttgccaACT-3'	---	---	<i>i, ii</i>
2	5'-GAGTtacttgccaACT-3'	3'-GBB-Am	NSP	<i>i</i>
3	5'-GAGTtacttgccaACT-3'	3'-C <sub>6</sub> SH	NMM	<i>i</i>
4	5'-GAGTtacttgccaACT-3'	3'-C <sub>6</sub> SH	NEM	<i>i</i>
5	5'-GN-AmC <sub>6</sub> -caGAGTtacttgccaACT-3'	---	---	<i>i, ii</i>
6	5'-GN-AmC <sub>6</sub> -caGAGTtacttgccaACT-3'	3'-C <sub>6</sub> SH	NEM	<i>i</i>
7	5'-GAGTtacttgccaACT-3'	3'-C <sub>6</sub> SH	[ <sup>3</sup> H]-NEM	<i>ii</i>
8	5'-GN-AmC <sub>6</sub> -caGAGTtacttgccaACT-3'	3'-C <sub>6</sub> SH	[ <sup>3</sup> H]-NEM	<i>ii</i>

(ASAGPR) expressed on the surface of hepatocytes (Sewing et al. 2019).

For a better clarification in this manuscript of individual ASO constructs, ASO-GalNAc conjugates, consisting of an *N*-acetylgalactosamine cluster with C<sub>6</sub>-amine-linker, as well as two DNA nucleotides (cytosine, adenine, acting as “cleavable linker”) at the 5'-end of the ASO sequence is referred to as “GalNAc”. The identical sequence without a GalNAc construct is referred to as “naked”. The term “tagged” describes ASOs conjugated with NSP, NEM, or NMM on amine- or thiol-linkers. “Untagged” refers to the unmodified ASO, without linker and label.

For an in vivo proof-of-concept study, Malat1 ASOs (naked and GalNAc) were synthesized as tritium analogs to demonstrate the value and applicability of our labeling approach in preclinical studies.

#### In vitro studies

The introduction of a tritium tag via a short linker is, relative to the entire oligonucleotide construct, an overall small chemical modification at the 3'-end. In general, it is not expected that the hybridization of the modified ASOs with the target will be significantly altered. However, in order to verify that the tagging can be used for in vivo studies, two key features must be met: metabolic stability and maintenance of the target interaction resulting in a similar potency as its untagged counterpart. The following in vitro studies show which conjugation technique



is suitable for an *in vivo* study in order to compare the modified tagged ASO with the untagged ASO.

#### Hepatocyte incubations and RNA measurements

The ability to decrease Malat1 RNA concentration levels was tested in primary mouse hepatocytes by adding the ASOs to the culture medium. After 3 h, the medium containing the ASOs was removed, the cells were washed, and then further incubated in fresh medium for 21 h and 69 h, respectively. Tagged naked ASOs 2 (NSP;  $IC_{50} = 60.1 \pm 6.3$  nM), 3 (NMM;  $IC_{50} = 70.0 \pm 6.3$  nM), and 4 (NEM;  $IC_{50} = 77.6 \pm 3.6$  nM) reduced Malat1 RNA levels after 24 h (Fig. 3A) similar to the untagged ASO 1 ( $IC_{50} = 74.3 \pm 9.1$  nM). After 72 h (Fig. 3B), the RNA level reduction was more pronounced than after 24 h. The untagged ASO 1 showed the highest Malat1 RNA reduction ( $IC_{50} = 11.2 \pm 3.2$  nM), ASO 2 (NSP;  $IC_{50} = 30.1 \pm 1.4$  nM), and 3 (NMM;  $IC_{50} = 25.6 \pm 1.2$  nM) were in a similar range, while ASO 4 was slightly less potent (NEM;  $IC_{50} = 54.3 \pm 2.9$  nM).

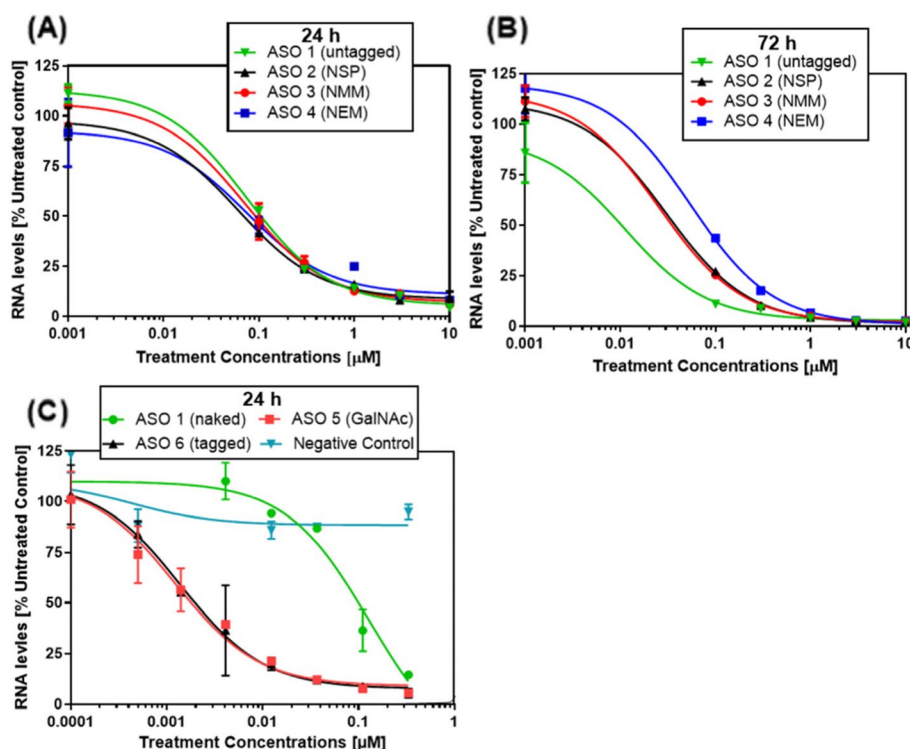
In addition to naked ASOs, GalNAc-conjugated ASO was also tagged with NEM on a 3'-end  $C_6$  thiol-linker (ASO 6). As expected, the GalNAc-conjugation increased target RNA level reduction compared to the naked ASO

1, while a negative control ASO targeting ApoB mRNA (Disterer et al. 2013) did not show reduction in Malat1 RNA levels. The NEM-tagged ASO 6 ( $IC_{50} = 1.40 \pm 0.10$  nM) showed a similar target reduction as the untagged ASO 5 ( $IC_{50} = 1.24 \pm 0.17$  nM) after 24 h (Fig. 3C). As the uptake of GalNAc-conjugated ASOs was faster than with naked ASOs, the focus was on the early time point at 24 h and the measurement after 72 h was not carried out. The results, however, indicate that the chemical modifications did not change the uptake of ASO into hepatocytes, and that target reduction potential was similar for tagged ASOs compared to their untagged counterpart.

#### Metabolite identification



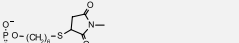
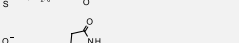
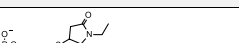

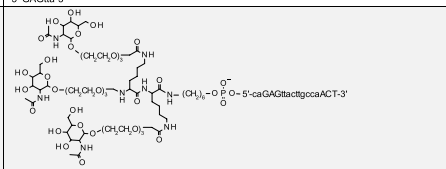
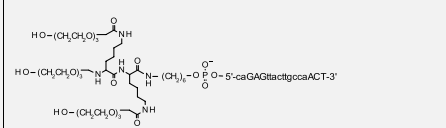


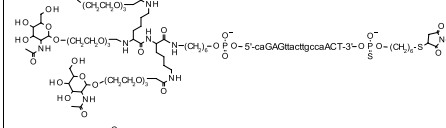
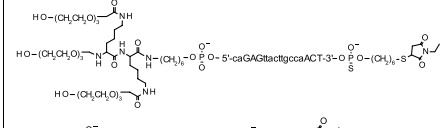
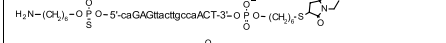
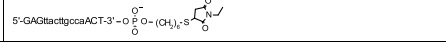
The stability towards degradation and metabolism was assessed for all ASOs after 3 h of incubation in primary mouse hepatocytes, followed by post-incubation periods of 21 h and 69 h, respectively. LC-HRMS was applied to an aliquot of the same mouse hepatocyte samples, which were used for target reduction assessment in order to identify the key cleavage products and/or metabolites.

Table 2 summarizes the results obtained for all ASOs investigated. Metabolite identification (MetID) experiments revealed that NSP-tagged ASO 2 showed



**Fig. 3** Concentration-dependent target reduction in mouse hepatocytes (*in vitro*) treated with NSP and maleimide-tagged naked ASOs and their untagged counterpart. Malat1 RNA levels were assessed after **A** 24 h and **B** 72 h. **C** Malat1 RNA levels of GalNAc-conjugated oligonucleotides compared with naked-Malat1 and negative-control ASO after 24 h (mean and SD,  $n=3$ )

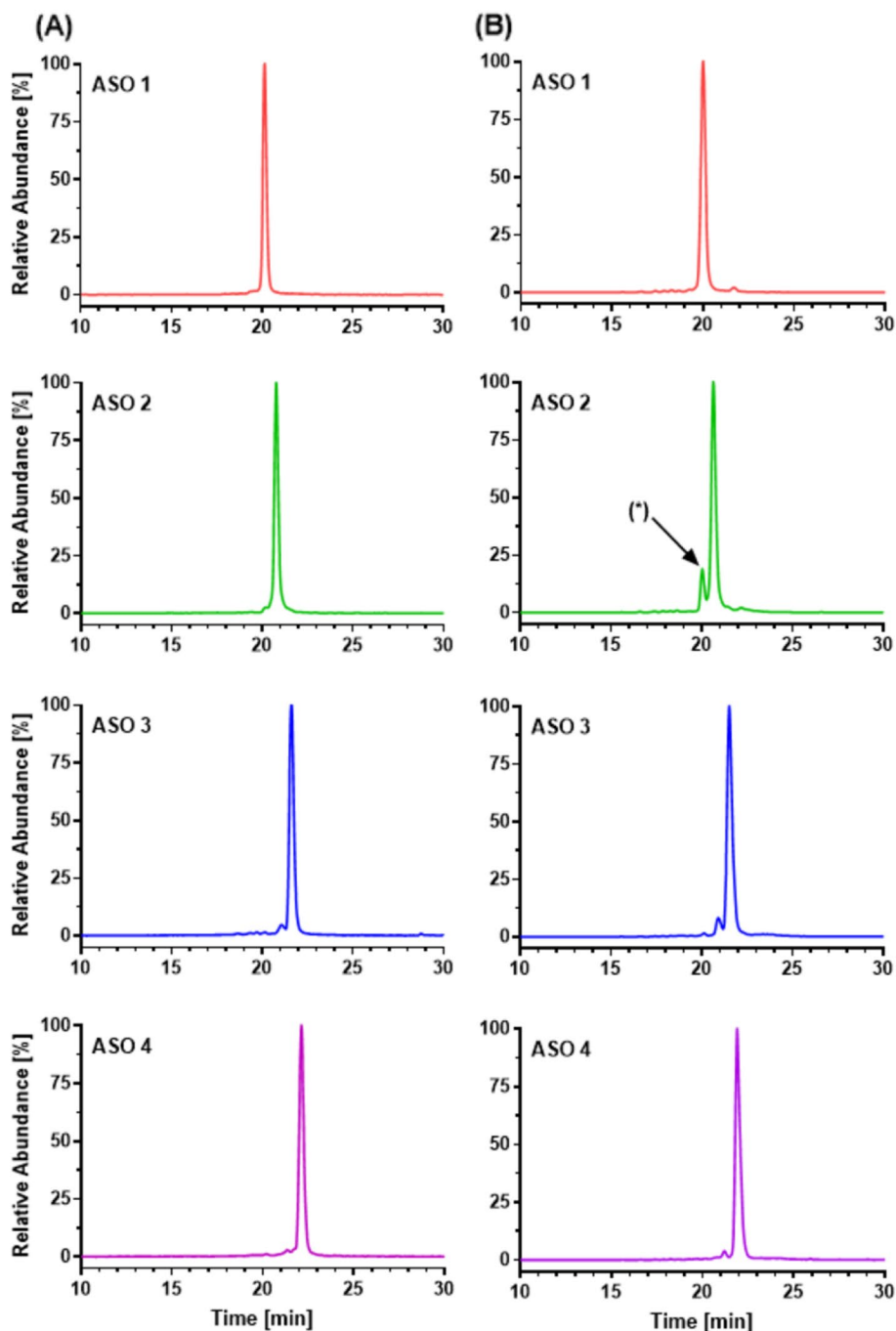
**Table 2** Degradation products for ASOs 1 to 6 from mouse hepatocyte metabolism identification study after 72 h of incubation. Capital letters in the oligonucleotide sequence describe LNA-modified nucleotides, and small letters describe DNA nucleotides. *n.d.* not detectable

ASO (Tag)	Oligonucleotide sequence 5' → 3'	Peak area [%]
1 (untagged)	5'-GAGtactgccaACT-3'	97.3
	5'-GAGtactgccaAC-3'	0.1
	5'-GAGtactgccaA-3'	n.d.
	5'-GAGtactgcca-3'	0.1
	5'-GAGtactgcca-3'	0.2
	5'-GAGtactgca-3'	0.3
	5'-GAGtactgc-3'	0.4
	5'-GAGtactg-3'	0.6
	5'-GAGtact-3'	0.5
	5'-GAGtac-3'	0.2
5'-GAGta-3'	0.1	
2 (NSP)	 $5'-GAGtactgccaACT-3' - O^-\text{P}(=O)(OH)O$	89.0
	 $5'-GAGtactgccaACT-3' - O^-\text{P}(=O)(OH)O$	5.9
	5'-GAGtactgccaACT-3'	2.6
	5'-GAGtactgccaAC-3'	n.d.
	5'-GAGtactgccaA-3'	n.d.
	5'-GAGtactgcca-3'	n.d.
	5'-GAGtactgcca-3'	0.2
	5'-GAGtactgca-3'	0.3
	5'-GAGtactgc-3'	0.4
	5'-GAGtactg-3'	0.6
	5'-GAGtact-3'	0.5
	5'-GAGtac-3'	0.3
	5'-GAGta-3'	0.1
3 (NMM)	 $5'-GAGtactgccaACT-3' - O^-\text{P}(=O)(OCH_3)O$	98.7
	 $5'-GAGtactgccaACT-3' - O^-\text{P}(=O)(OCH_3)O$	n.d.
	5'-GAGtactgccaACT-3'	0.2
	5'-GAGtactgccaAC-3'	n.d.
	5'-GAGtactgccaA-3'	n.d.
	5'-GAGtactgcca-3'	n.d.
	5'-GAGtactgcca-3'	0.1
	5'-GAGtactgca-3'	0.1
	5'-GAGtactgc-3'	0.2
	5'-GAGtactg-3'	0.3
	5'-GAGtact-3'	0.2
	5'-GAGtac-3'	0.1
	5'-GAGta-3'	n.d.
4 (NEM)	 $5'-GAGtactgccaACT-3' - O^-\text{P}(=O)(OCH_3)O$	99.0
	 $5'-GAGtactgccaACT-3' - O^-\text{P}(=O)(OCH_3)O$	n.d.
	5'-GAGtactgccaACT-3'	n.d.
	5'-GAGtactgccaAC-3'	n.d.
	5'-GAGtactgccaA-3'	n.d.
	5'-GAGtactgcca-3'	n.d.
	5'-GAGtactgcca-3'	0.1
	5'-GAGtactgca-3'	0.1
	5'-GAGtactgc-3'	0.1
	5'-GAGtactg-3'	0.1
	5'-GAGtact-3'	0.3
	5'-GAGtac-3'	0.2
	5'-GAGtac-3'	0.1
5'-GAGta-3'	n.d.	
5 (GalNAc-conjugated, untagged)	 $H_2N-(CH_2)_6-O^-\text{P}(=O)(OCH_3)O-5'-caGAGtactgccaACT-3'$	47.2
	 $H_2N-(CH_2)_6-O^-\text{P}(=O)(OCH_3)O-5'-caGAGtactgccaACT-3'$	3.5
	 $H_2N-(CH_2)_6-O^-\text{P}(=O)(OCH_3)O-5'-caGAGtactgccaACT-3'$	2.6
	5'-GAGtactgccaACT-3'	46.2
	 $H_2N-(CH_2)_6-O^-\text{P}(=O)(OCH_3)O-5'-caGAGtactgccaACT-3'$	2.3
6 (GalNAc-conjugated, NEM)	 $H_2N-(CH_2)_6-O^-\text{P}(=O)(OCH_3)O-5'-caGAGtactgccaACT-3'-O^-\text{P}(=O)(OCH_3)O$	45.2
	 $H_2N-(CH_2)_6-O^-\text{P}(=O)(OCH_3)O-5'-caGAGtactgccaACT-3'-O^-\text{P}(=O)(OCH_3)O$	2.2
	 $H_2N-(CH_2)_6-O^-\text{P}(=O)(OCH_3)O-5'-caGAGtactgccaACT-3'-O^-\text{P}(=O)(OCH_3)O$	2.3
	 $5'-GAGtactgccaACT-3'-O^-\text{P}(=O)(OCH_3)O$	50.3

instability with 11% of loss due to cleavage of the propionate and additionally by cleavage of the aminopropyl glycerol-linker at the 3'-end after 72 h.

In contrast, ASOs tagged by NMM and NEM in mouse hepatocytes cells were almost unchanged for

up to 72 h according to the LC-HRMS measurements. No relevant tag instability or metabolite formation was observed in the generic *all-ion fragmentation* (AIF) mass-chromatograms (Fig. 4A, B).



**Fig. 4** HPLC measurements (AIF, normalized) of naked ASO constructs from the MetID study. From the top: ASO 1 (untagged), ASO 2 (NSP), ASO 3 (NMM), and ASO 4 (NEM). **A** Reference compounds. **B** After 72 h incubation in primary mouse hepatocytes. (\*) Arrow indicates the undesired degradation product of hydrolysis, which results to the loss of the tag

The untagged GalNAc-ASO 5 and the corresponding NEM-tagged ASO 6 showed several metabolites in mouse hepatocytes mainly driven by the desired release of the naked ASO resulting from hydrolysis of the two diphosphate-linked nucleotide part (“cleavable linker”) and cleavages within the triantennary GalNAc construct. No undesired instability of the tag was observed. The main metabolites contained the maleimide derivative, demonstrating the applicability of using NEM to introduce tritium into ASOs. Therefore, the synthesis of tritium-labeled ASO for use in a proof-of-concept in vivo mouse study was pursued.

### In vivo mouse study

PK studies in mice were conducted using [<sup>3</sup>H]-NEM-modified Malat1-based ASOs and their untagged counterparts. After a single subcutaneous dose of 1 mg/kg of body weight of untagged ASOs 1 (naked) and 5 (GalNAc), and their counterparts tagged with [<sup>3</sup>H]-NEM: ASOs 7 (naked) and 8 (GalNAc), the concentrations in tissues (liver, kidney, spleen) were determined. Plasma concentrations and the recovery rate in urine and feces were monitored with the tritium-tagged ASOs. The most abundant metabolites were identified from the urine samples. In addition, the RNA levels after in vivo

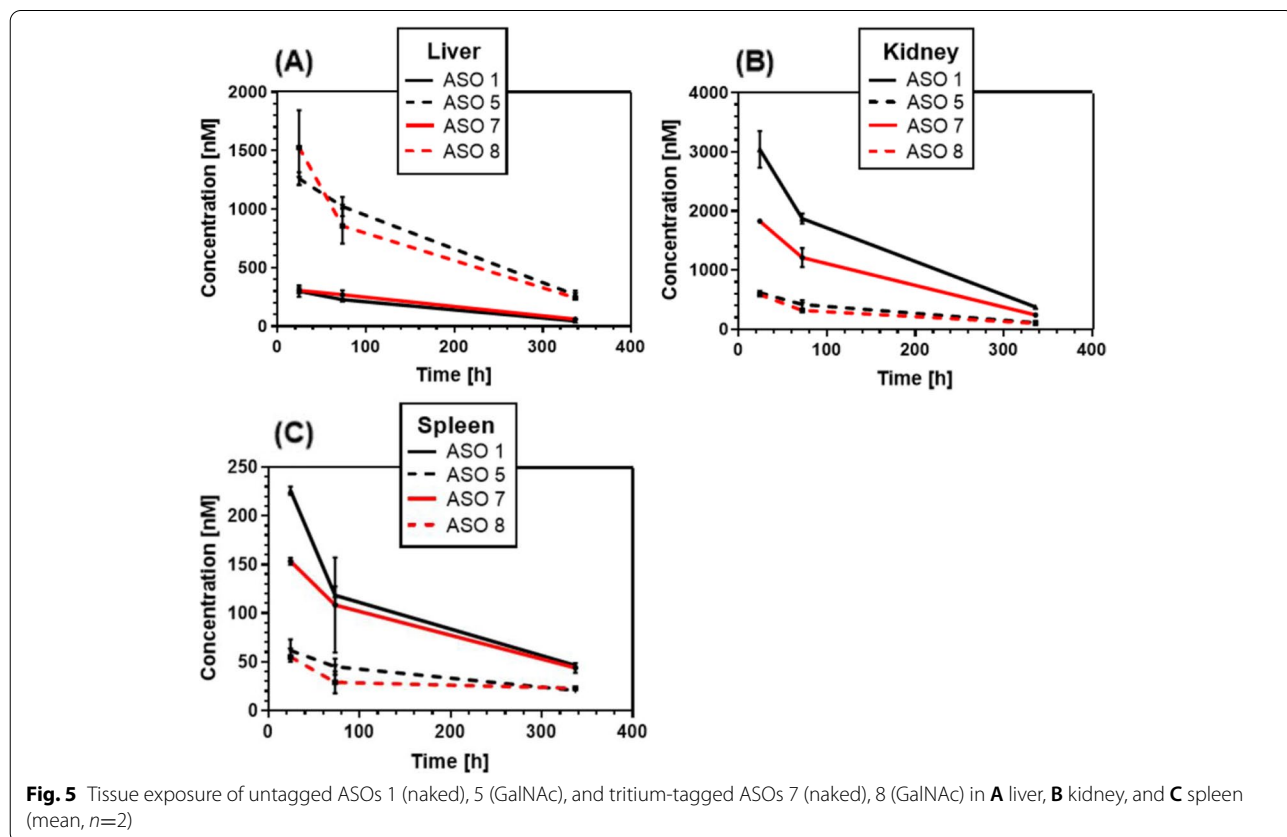
inhibition in tissues of tagged-ASOs and untagged counterparts were compared.

### Tissue concentrations in liver, kidney, and spleen

Liver, kidney, and spleen tissues were collected after 1 day, 3 days, and 14 days, and concentrations were determined for tritium-labeled ASOs by LSC or LC-MS/MS for untagged ASOs (Fig. 5). As expected, GalNAc-conjugated ASOs of both untagged and tritium-tagged ASOs resulted in increased liver concentrations compared to their naked counterparts. The highest concentrations of naked ASOs were found in the kidney. For all tissues, the results obtained for the tagged vs untagged counterparts were comparable, which indicates a similar distribution in the respective examined tissues, liver, kidney, and spleen.

### Metabolism

Metabolic profiles were assessed using urine samples collected in the time interval from 0 to 24 h after administration. The main product in both cases, ASOs 7 and 8, was identified as the naked ASO-construct. In addition, several metabolites were observed at detectable signal intensities. A summary of the results is shown in Table 3. The metabolites found were mainly formed by hydrolysis



**Table 3** Most abundant metabolites observed in urine of mice from 0 to 24 h after a single dose of [<sup>3</sup>H]-NEM-labeled ASOs 7 and 8. Capital letters in the oligonucleotide sequence describe LNA-modified nucleosides, and small letters describe DNA nucleosides. *n.d.* not detectable

ASO (Tag)	Oligonucleotide sequence 5' → 3'	MS Peak Area [%]
7 ([ <sup>3</sup> H]-NEM)		1
		29
		56
		14
8 (GalNAc-conjugated [ <sup>3</sup> H]-NEM)		<i>n.d.</i>
		12
		39
		20
		29

of the phosphorothioate backbone, which resulted in shorter oligomers and confirmed the results of *in vitro* experiments. The metabolites identified in the liver, kidney, and spleen are consistent with the main mode of ASO metabolism being initial endonuclease-mediated hydrolysis at positions within the DNA chain of the parent compound, and by subsequent exonuclease mediated hydrolysis resulting in shorter metabolites.

#### Plasma and excreta

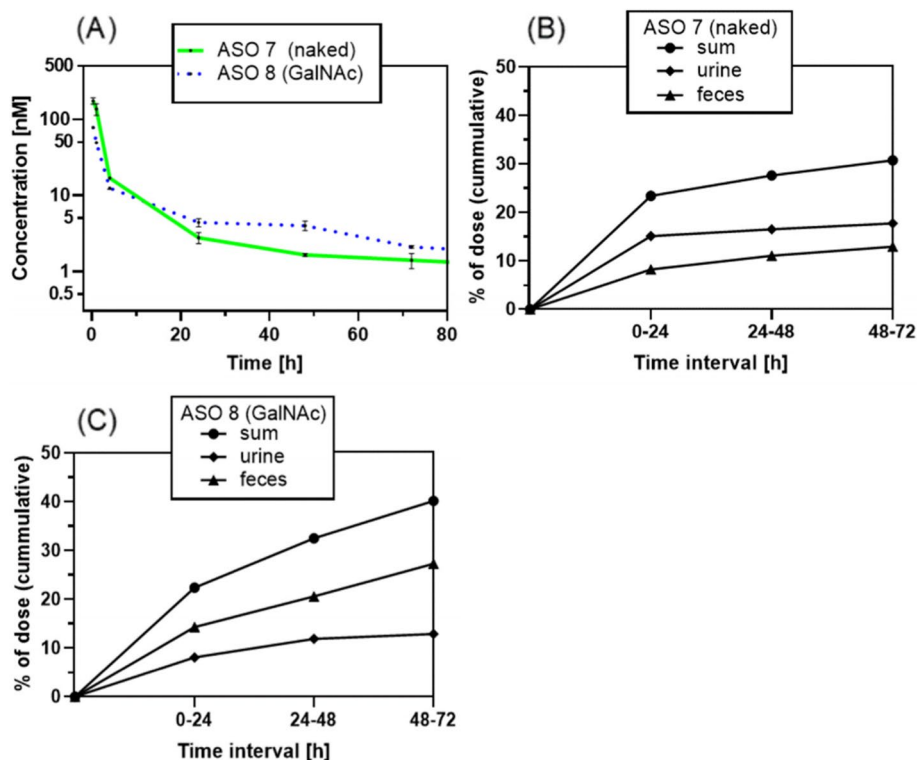
The mean plasma concentration-time curves are shown in Fig. 6A as determined by LSC for [<sup>3</sup>H]-labeled ASOs. Both tritium-labeled ASOs, naked and GalNAc, have a typically fast distribution phase. Plasma levels peaked at the first sampling time point. At 15 min after subcutaneous administration of 1 mg/kg of body weight of ASOs 7 (naked) and ASO 8 (GalNAc) in two animals, the mean maximum plasma concentration was 175 nM and 78 nM, respectively.

The major part of the radioactive dose was recovered within the first 24 h. Twenty-four percent of the dose

was collected of ASO 7, and 23% of ASO 8. The contribution of the subsequent collection periods up to 72 h was only small for naked ASO 7 with an overall recovery of 32%. For GalNAc ASO 8, the overall recovery was 41% of the dose (Fig. 6B, C).

#### Malat1 RNA levels after *in vivo* inhibition

Next, the inhibitory effect of ASO exposure on Malat1-RNA levels in liver, kidney, and spleen was investigated after 1 day, 3 days, and 14 days. In the liver, a reduction of the RNA levels in the range of 5–12%, compared with untreated saline, was observed at each time point for all four ASOs. In kidney, the effect was slightly more pronounced, in particular for the tagged ASOs (naked and GalNAc), which showed a reduction in Malat1 RNA levels in the range of 5 to 20% and in 25–38% of their untagged counterparts. In spleen, no significant change in Malat1 RNA levels was observed after treatment with any ASO used in this study (Fig. 7A–C).



**Fig. 6** **A** Plasma concentration-time profile of  $[^3\text{H}]$ -labeled ASO 7 (naked) and  $[^3\text{H}]$ -labeled ASO 8 (GalNAc). **B, C** Excretion through urine and feces (mean,  $n=2$ )

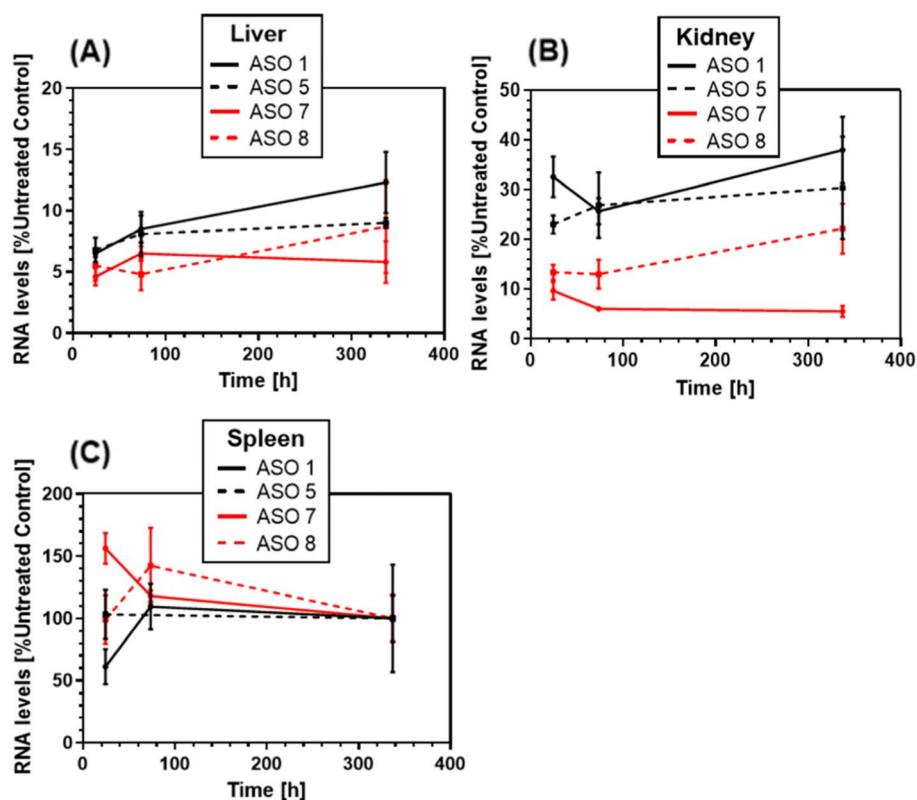
## Discussion

Investigating ADME characteristics of new small molecule drugs using radiolabeled drugs is well established as it enables reliable quantification, traceability, and the generation of excretory mass balance data of the drug molecules, even after being transformed into various metabolites. For ASO drugs, however, the labeling with radioisotopes is far less established. The synthesis of radiolabeled ASO drugs is generally more complex and, despite the increasing importance of therapeutic ASOs in pre-clinical and clinical research, simple, straightforward chemical synthesis approaches to introduce radioisotopes into ASOs that achieve sufficient specific activity are not readily available. Therefore, we explored new approaches using *N*-succinimidyl propionate and maleimide-derivatives for a potential tritium-introduction into ASOs. Initially, NSP was used to introduce propionyl to the 3'-end. Conjugations at the 3'-end of amino linkers are known in the literature. Buntz and co-workers (Buntz et al. 2019) have reported conjugations of NHS-activated fluorescent labels to amino-modified oligonucleotides. Thus, an analogy to the smaller NSP, compared to fluorescent dyes, appears to be a feasible technique for labeling ASOs with tritium. Despite being synthetically favorable, the tagged ASO resulting from this approach

was unstable and showed considerable cleavage with the introduced propionate, resulting in loss of isotopic tag. This approach was therefore not further pursued. The second approach using NEM resulted in 3'-end tagged ASOs that were shown to be stable in vitro while maintaining the target affinity. Consequently, this conjugation approach was used to synthesize  $[^3\text{H}]$ -NEM analogs to be applied in proof-of-concept studies in mice to demonstrate the applicability in in vivo studies.

Hydrolysis by 3'-exonucleases may contribute to the instability of ASOs and 3'-end labeling could therefore result in label loss. For the ASOs used in this study for maleimide 3'-labeling, we could demonstrate that the 3'-end was largely stable against 3'-exonuclease activity. In cases of different ASOs where 3'-exonuclease activity is contributing significantly to instability, the 3'-end labeling approach shown here might be limited. For such cases, however, we assume that the conjugation concept can also be carried out on thiol-based linkers at 5'-end, as preliminary data already suggest with similar types of tritium-labeled maleimides (Edelmann and Muser 2021).

In our study, we focused on the 3'-end, as the aim was to use modifications with GalNAc attached to the 5'-end of the ASO. In addition, ASOs are typically optimized to prevent exonuclease degradation as this improves the



**Fig. 7** Malat1 RNA levels after in vivo inhibition of ASOs 1 (naked), 5 (GalNAc), and [ $^3\text{H}$ ]-labeled ASO 7 (naked), 8 (GalNAc) in liver (A), kidney (B), and spleen (C) (mean,  $n=2$ )

overall ADME properties. The decision as to whether the label is attached to the 5'-end or 3'-end eventually depends on the stability of the oligonucleotide 3'-end and of other conjugation interests, e.g., GalNAc conjugation. In this regard, an in vitro assessment of ASO uptake, target reduction, and metabolic stability could inform the selection of the best possible labeling position.

Known issues in the tritium-labeling of ASOs are related to the number of synthesis steps, which are associated with poor yields and low specific activity. For both factors, the approach shown here is beneficial, as only one principal modification step is required with the commercially available radioactive precursor [ $^3\text{H}$ ]-NEM. The specific activity achievable (up to 17 Ci/mmol) is, to the best of our knowledge (Post et al. 2019; Yu et al. 2007; Christensen et al. 2012; Graham et al. 1993), the highest specific activity that has been obtained so far with a tritiated oligonucleotide for use in in vivo studies. An even higher specific activity of the desired ASOs could be achieved by using more optimized maleimide derivatives with higher specific activity or by using more equivalents of tritium-labeled maleimide starting material (in contrast to an excess of oligonucleotides). The resulting specific activities in our study, however, still comfortably

meet the requirements for in vivo disposition studies. In order to demonstrate the applicability of the labeling method for conducting in vivo studies with ASOs, mice were treated with a single dose of ASOs 7 and 8. In the collection periods up to 72 h for naked ASO 7, an overall recovery of 32% and for GalNAc ASO 8 an overall recovery of 41% of the dose was found. The main proportion of radioactivity was recovered in urine, slightly less in feces. This is in line with literature reports that renal excretion is the dominant route of elimination for ASOs (Bosgra et al. 2019; Yu et al. 2007). Therefore, tritiated oligonucleotides labeled using this described conjugation technique might be well suited for mass balance and quantitative whole body autoradiography studies in order to gain a better understanding of the distribution and excretion of potential therapeutic ASOs.

## Conclusions

Novel approaches to labeled antisense oligonucleotides with  $^3\text{H}$  were described. of *N*-Succinimidyl propionate (NSP) was conjugated to an amino-linker at the 3'-end, and *N*-methylmaleimide (NMM) and *N*-ethylmaleimide (NEM) were conjugated Michael addition to sulfhydryl-linkers of oligonucleotides that target Malat1. Based on

non-radiolabeled (cold) Malat1-ASO examples, in vitro experiments were carried out to investigate target efficiency and stability after the tag-modification. All cold-tagged Malat1 oligonucleotides showed similar RNA target reduction after 24 h, but metabolic instability of tag and linker in mouse hepatocyte cells was observed for the NSP-tagged ASO.

In contrast, the maleimide conjugates were metabolically stable in vitro up to 72 h. Consequently, [<sup>3</sup>H]-NEM was selected as the conjugation agent of choice for this study, resulting in tritium-labeled ASO with high molar specific activity of up to 17 Ci/mmol. A single-dose PK experiment, including [<sup>3</sup>H]-NEM-tagged GalNAc and naked ASO constructs, was performed in mice. It was demonstrated that the radiolabeled ASOs, despite the maleimide conjugation, show an equivalent PK behavior as their congeners. In conclusion, this new method to efficiently conjugate pre-labeled tags provides a powerful technique for fast and safe access to tritium-labeled oligonucleotides, e.g., for preclinical pharmacokinetic or autoradiography studies.

#### Acknowledgements

The authors acknowledge the contribution from Dr. Michael B. Ottener, Dr. Filippo Sladojevich, and Dr. Thomas Hartung from Roche Innovation Center Basel (RICB) as well as Prof. Stephen M. Husbands and Dr. Ian S. Blagbrough from the University of Bath for providing valuable comments on the manuscript, and Jon Kyle Bodnar for thorough review and language editing of the manuscript. We are also grateful to Thorsten Muser (RICB) for contribution of conjugation experiments, Pawel Dzygiel (RICB) for mass spectrometry bioanalysis, and Peter Schrag (RICB) for his support with in vivo experiments.

#### Authors' contributions

Wrote or contributed to the writing of the manuscript: MRE, CH, CS, EK, AB. Conjugation concept and synthesis: MRE. In vitro studies and data analyses and interpretation: CH, MBD, EK, AB. In vivo PK study and data analyses and interpretation: CH, MBD, GF, CS, EK, AB. The authors read and approved the final manuscript.

#### Authors' information

*Martin R. Edelmann, Engineer (FH):*

Martin studied biological chemistry at the University of Applied Sciences in Mannheim, Germany and completed his diploma thesis in 2006 at Novartis Pharma, Switzerland. After 4 years of research in medicinal chemistry at the Novartis Institutes for BioMedical Research, he moved to F. Hoffmann-La Roche's Isotope Synthesis Laboratory as a Senior Scientist. Martin is responsible for radiolabeling of small molecules, oligonucleotides, and proteins with carbon-14 and tritium. In January 2020, he started his doctorate at the University of Bath, UK, in the Department of Pharmacy & Pharmacology under the supervision of Dr. Ian S. Blagbrough and Prof. Stephen M. Husbands (University of Bath, UK) as well as Dr. Michael B. Ottener and Dr. Filippo Sladojevich (Roche).

*Christophe Husser, Engineer (FH):*

Christophe Husser works as a Scientist within Pharmaceutical Sciences focused on Drug Metabolism and High Resolution Mass Spectrometry. After his studies at the University of Strasbourg, France, and at the University of Applied Sciences in Aalen, Germany, he received a technology degree in chemistry and an Engineer degree in analytical chemistry. At F. Hoffmann-La Roche, his responsibilities and interests are in the area of drug biotransformation from therapeutic proteins and oligonucleotides.

*Martina B. Duschmalé, M.Sc.:*

Martina B. Duschmalé received her Master's degree in Biomedical Sciences at the University of Applied Science in Albstadt-Sigmaringen, Germany. During her master's thesis in 2013 at F. Hoffmann-La Roche, Switzerland, she

investigated the evaluation of models for predicting Drug-Drug Interactions. Martina has been Vice President of the Basler Wirrgarten Foundation since 2019 and President of the Wibrandis Foundation in Basel, Switzerland since 2020.

*Guy Fischer, BTS:*

Guy Fischer works as a Scientist in Bioanalytical R&D and focuses on the characterization of small molecules and oligonucleotides. In 1978, he received a higher technician certificate in biochemistry (Brevet de technicien supérieur) from the Académie de Strasbourg, France. His technology expertise covers a wide range of analyses, including quantitative measurements in biological matrices of various species.

*Claudia Senn, Ph.D.:*

Claudia Senn works as a Principal Scientist and Leader in the Translational Pharmacology and Toxicology Group, leading preclinical in vivo studies for pharmacokinetic and safety assessment. She received her Ph.D. in 2001 in the field of Biosynthesis of Neural Structure in the Center for Molecular Neurobiology Hamburg, Germany.

*Erich Koller, Ph.D.:*

Erich Koller works as a Senior Principal Scientist within Pharmaceutical Sciences focused on drug metabolism, pharmacokinetics, and pharmacodynamics. After his studies of biochemistry, he received his Ph.D. in 1992 in biochemistry from the ETH in Zurich. He then did his postdoctoral studies at the Sanford Burnham Prebys Medical Discovery Institute in La Jolla, CA. He then joined Ionis Pharmaceuticals in Carlsbad, CA. In 2014, he moved back to Switzerland where he joined F. Hoffmann-La Roche.

*Andreas Brink, Ph.D.:*

Andreas Brink works as a Senior Principal Scientist within Pharmaceutical Sciences focused on Drug Metabolism and High Resolution Mass Spectrometry. After his studies of chemistry and biology, he received his Ph.D. in 2007 in the field of genetic toxicology at the Department of Toxicology and Pharmacology of the University Würzburg, Germany. At F. Hoffmann-La Roche, his responsibilities and interests are in the area of drug biotransformation, from early drug discovery to drug development (e.g. metabolite identification, reactive metabolites, MIST assessment for small molecules) including biotransformation of oligonucleotides.

#### Funding

The authors received no funding for this article.

#### Availability of data and materials

The datasets used and/or analyzed during the current study are available from the corresponding author on reasonable request.

#### Declarations

#### Competing interests

F. Hoffmann-La Roche AG has submitted a patent application (WO2019/145384) covering the conjugation process of oligonucleotides with [<sup>3</sup>H]-labeled maleimide derivatives.

#### Author details

<sup>1</sup>Department of Pharmacy and Pharmacology, University of Bath, Bath BA2 7AY, UK. <sup>2</sup>Roche Pharma Research and Early Development, Therapeutic Modalities, Roche Innovation Center Basel, F. Hoffmann-La Roche Ltd, Grenzachstr. 124, CH-4070 Basel, Switzerland. <sup>3</sup>Roche Pharma Research and Early Development, Pharmaceutical Sciences, Roche Innovation Center Basel, F. Hoffmann-La Roche Ltd, CH-4070 Basel, Switzerland.

Received: 2 July 2021 Accepted: 21 October 2021

Published online: 15 November 2021

#### References

- Bosgra S, Sipkens J, de Kimpe S, den Besten C, Datson N, van Deutekom J (2019) The pharmacokinetics of 2'-O-methyl phosphorothioate antisense oligonucleotides: experiences from developing exon skipping therapies for Duchenne muscular dystrophy. *Nucleic Acid Ther* 29(6):305–322
- Buntz A, Killian T, Schmid D, Seul H, Brinkmann U, Ravn J et al (2019) Quantitative fluorescence imaging determines the absolute number of locked



- nucleic acid oligonucleotides needed for suppression of target gene expression. *Nucleic Acids Res* 47(2):953–969
- Christensen J, Natt F, Hunziker J, Krauser J, Andres H, Swart P (2012) Tritium labeling of full-length small interfering RNAs. *J Labelled Comp. Radiopharm* 55(6):189–196
- Disterer P, Al-Shawi R, Ellmerich S, Waddington SN, Owen JS, Simons JP et al (2013) Exon skipping of hepatic APOB pre-mRNA with splice-switching oligonucleotides reduces LDL cholesterol in vivo. *Mol Ther* 21(3):602–609
- Edelmann MR, Muser T (2021) Tritium O-methylation of N-alkoxy maleimide derivatives as labeling reagents for biomolecules. *Bioconjug Chem* 32(5):1027–1033
- Graham M, Freier S, Crooke R, Ecker D, Maslova R, Lesnik E (1993) Tritium labeling of antisense oligonucleotides by exchange with tritiated water. *Nucleic Acids Res* 21(16):3737–3743
- Grünweiler A, Hartmann RK (2007) Locked nucleic acid oligonucleotides. *BioDrugs* 21(4):235–243
- Hagedorn PH, Persson R, Funder ED, Albæk N, Diemer SL, Hansen DJ et al (2018) Locked nucleic acid: modality, diversity, and drug discovery. *Drug Discovery Today* 23(1):101–114
- Havens MA, Hastings ML (2016) Splice-switching antisense oligonucleotides as therapeutic drugs. *Nucleic Acids Res* 44(14):6549–6563
- Husser C, Brink A, Zell M, Müller MB, Koller E, Schadt S (2017) Identification of GalNAc-conjugated antisense oligonucleotide metabolites using an untargeted and generic approach based on high resolution mass spectrometry. *Anal Chem* 89(12):6821–6826
- Husser C, Koller E, Brink A, Schadt S (2019) Studying the biotransformation of phosphorothioate-containing oligonucleotide drugs by LC-MS. In: Gissberg O, Zain R, Lundin KE (eds) *Oligonucleotide-Based Therapies*. Springer, Berlin, pp 307–315
- Muntoni F, Wood MJ (2011) Targeting RNA to treat neuromuscular disease. *Nat Rev Drug Discov* 10(8):621–637
- Palazzolo A, Feuillastre S, Pfeifer V, Garcia-Argote S, Bouzouita D, Tricard S et al (2019) Efficient access to deuterated and tritiated nucleobase pharmaceuticals and oligonucleotides using hydrogen-isotope exchange. *Angew Chem* 131(15):4945–4949
- Post N, Yu R, Greenlee S, Gaus H, Hurh E, Matson J et al (2019) Metabolism and disposition of volanesorsen, a 2'-O-(2-methoxyethyl) antisense oligonucleotide, across species. *Drug Metab Dispos* 47(10):1164–1173
- Sasaki S, Sun R, Bui HH, Crosby JR, Monia BP, Guo SL (2019) Steric inhibition of 5' UTR regulatory elements results in upregulation of human CFTR. *Mol Ther* 27(10):1749–1757. <https://doi.org/10.1016/j.ymthe.2019.06.016>
- Sewing S, Boess F, Moisan A, Bertinetti-Lapatki C, Minz T, Hedtjaern M et al (2016) Establishment of a predictive in vitro assay for assessment of the hepatotoxic potential of oligonucleotide drugs. *PLoS One* 11(7):e0159431
- Sewing S, Gubler M, Gérard R, Avignon B, Mueller Y, Braendli-Baiocco A et al (2019) GalNAc conjugation attenuates the cytotoxicity of antisense oligonucleotide drugs in renal tubular cells. *Mol Ther Nucleic Acids* 14:67–79
- Shemesh CS, Rosie ZY, Gaus HJ, Greenlee S, Post N, Schmidt K et al (2016) Elucidation of the biotransformation pathways of a Galnac3-conjugated antisense oligonucleotide in rats and monkeys. *Mol Ther Nucleic Acids* 5:e319
- Stephenson ML, Zamecnik PC (1978) Inhibition of Rous sarcoma viral RNA translation by a specific oligodeoxyribonucleotide. *Proc Natl Acad Sci USA* 75(1):285–288
- Straarup EM, Fisker N, Hedtjærn M, Lindholm MW, Rosenbohm C, Aarup V et al (2010) Short locked nucleic acid antisense oligonucleotides potently reduce apolipoprotein B mRNA and serum cholesterol in mice and non-human primates. *Nucleic Acids Res* 38(20):7100–7111
- Tan, W., Iyer, R. P., Jiang, Z., Yu, D., & Agrawal, S. (1997). Method of tritium labeling oligonucleotides. Patent US5668262A, 16 Sept 1997
- Wang F, Zuroske T, Watts J (2020) RNA therapeutics on the rise. *Nat Rev Drug Discov* 19:441–442. <https://doi.org/10.1038/d41573-020-00078-0>
- Yu RZ, Kim T-W, Hong A, Watanabe TA, Gaus HJ, Geary RS (2007) Cross-species pharmacokinetic comparison from mouse to man of a second-generation antisense oligonucleotide, ISIS 301012, targeting human apolipoprotein B-100. *Drug Metab Dispos* 35(3):460–468

### Publisher's Note

Springer Nature remains neutral with regard to jurisdictional claims in published maps and institutional affiliations.

Submit your manuscript to a SpringerOpen® journal and benefit from:

- Convenient online submission
- Rigorous peer review
- Open access: articles freely available online
- High visibility within the field
- Retaining the copyright to your article

Submit your next manuscript at ► [springeropen.com](https://www.springeropen.com)